



TECH NOTE NO: 24  
TITLE: FRACTURE MECHANICS ANALYSIS FOR SAW CUTTING REQUIREMENTS OF CONCRETE PAVEMENTS  
AUTHORS: S. Villalobos, M.C. Gaedicke, Drs. J. Roesler & D. Lange  
Ph: (217)333-7835, Email: mgaedic2@uiuc.edu  
CONTACT: University of Illinois, Dept of Civil & Environmental Engineering  
1211 NCEL, MC-250, Urbana, IL 61801  
DATE/REV: 08/29/06

---

### **EXECUTIVE SUMMARY**

Concrete sawing operations are performed at pre-determined locations within the first 24 hours to prevent random cracking on jointed plain concrete pavements. In current construction procedures, the depth and the timing of the saw is usually established by the contractor based on experience. The objective of this study was to analyze the effect of several concrete mixture proportions and constituents on the early-age fracture properties and their effect on saw cut timing and depth for concrete pavements with several slab geometries. Concrete pavement mixtures with different coarse aggregate size and cementitious content were evaluated to determine the sensitivity of the measured fracture properties on saw cut model predictions. Finite element analysis was used to derive the geometric correction factors necessary to characterize the fracture properties of concrete based on the wedge plitting test configuration. A saw cut depth model proposed by Zollinger was modified to determine the timing and depth of notches on jointed plain concrete pavements. The theoretical analysis and practical example lead to the observation that if greater time is desired before saw cutting, the design should favor concrete materials with slower development of fracture properties. Larger coarse aggregate tends to increase concrete fracture toughness, and therefore will require deeper saw cuts. Thinner concrete pavements also require significantly deeper notch depth ratios relative to thicker slabs.

## INTRODUCTION

Concrete sawing operations are performed at pre-determined locations within the first 24 hours to prevent random cracking on jointed plain concrete pavements. Early age volumetric contractions due reductions in the internal concrete temperature and moisture will cause cracking in the concrete as a result of the concrete support layer restraint. In current construction procedures, the depth of the saw cuts is specified between one third and one quarter of the total depth of the pavement [1]. The proper time to perform the saw cutting of the concrete pavement is usually established by the contractor or field engineer based on experience.

Zollinger et al. [2,3] have developed an approach to calculate the saw cut depth and timing based on the fracture properties of concrete pavement mixtures [4-6]. The fracture mechanics-based model [2,3] uses the size effect model [7], to calculate the required notch depth at a given time and applied far-field stress. The size effect model integrates the measured concrete fracture properties, slab geometry, and boundary conditions into the determination of the concrete slab's nominal strength. The size effect model also accounts for the known specimen size effect exhibited by quasi-brittle such as concrete; that is, thinner concrete specimens are nominally stronger than thicker specimens.

The model proposed by Zollinger et al. provides a solid scientific basis to determine the appropriate saw cutting parameters for different pavement structures, but it requires early-age fracture properties such as the *Critical Stress Intensity Factor* ( $K_{IC}$ ) and *Critical Crack Extension* ( $c_f$ ) [2,3]. Early-age concrete fracture properties are especially difficult to obtain especially using the three point bending beam test (TPB) since the specimen's self weight significantly contributes to the peak load in the first 24 hours. A fracture test that has been found effective in determining the fracture properties of concrete at early ages is the Wedge Splitting Test (WST), which was first proposed by Tschegg [8] and further developed by Brürwiler and Wittman [9], and Østergaard [10]. The advantages of the WST over other fracture specimen types are it doesn't require complex equipment, minimizes the effect of the specimen self weight, has a large fracture area, and uses less concrete material per specimen compared with the TPB specimen. The WST is preferred for characterizing early-age fracture properties, however existing literature don't provide a method to calculate  $K_{IC}$  and  $c_f$  on WST samples.

## RESEARCH OBJECTIVES

The objective of this study is to analyze the effect of several concrete mixture proportions and constituents on the early-age fracture properties and their effect on saw cut timing and depth for concrete pavements with different slab geometries. Several concrete pavement mixtures with two coarse aggregate sizes and cementitious contents are evaluated to determine the sensitivity of the measured fracture properties on saw cut model predictions. The finite element method is used to derive the geometric correction factors necessary to characterize the fracture properties of concrete (*Critical Stress Intensity Factor* ( $K_{IC}$ ) and *Critical Crack Extension* ( $c_f$ )) based on the WST configuration and a modification to the two parameter fracture model procedure (Jenq and Shah ) [11]. The saw cut depth model proposed by Zollinger [2,3] is then modified to determine the

timing and depth of notches on jointed plain concrete pavements to minimize random cracking.

## EXPERIMENTAL PROGRAM

### *Experimental Design*

An experimental program was designed to analyze the effect of coarse aggregate size and cementitious content on the early-age concrete fracture properties and the required saw cut depth for jointed plain concrete pavements with 190 and 380 mm slab thickness. Table 1 lists the four concrete mixtures cast for this research. Two higher cementitious content mixtures (349 kg/m<sup>3</sup>) had a water-cementitious ratio of 0.38 with one containing 38 mm coarse aggregate size (identified as 688.38) and the other using 25 mm coarse size aggregate size (identified as 688.38st). Two lower cementitious mixtures (270 kg/m<sup>3</sup>) were prepared with a water-cementitious ratio of 0.44 and 38 and 25 mm coarse aggregate sizes, identified as 555.44 and 555.44st, respectively. Additional information about these mixtures can be found in Roesler et al. [12,13].

Wedge Splitting Test specimens were prepared for each of the mixtures in Table 1 for fracture testing at 6, 8, 10, 12 and 24 hours. Standard fresh (i.e., slump, air) and hardened concrete tests (i.e. 1, 3, 28 day compressive strength and modulus of elasticity) were performed on the specimens to verify the quality of the mixtures.

Table 1. Mixture design

ID	Units	555.44	555.44 st	688.38	688.38 st
w/cm		0.44		0.38	
Max aggregate size	mm (inch)	38 (1 1/2")	25 (1")	38 (1 1/2")	25 (1")
Water	kg/m <sup>3</sup>	145	145	155	155
Cement	kg/m <sup>3</sup>	270	270	349	349
Fly ash	kg/m <sup>3</sup>	59	59	59	59
Coarse Aggregate (SSD)	kg/m <sup>3</sup>	1152	1142	1093	1098
Fine Aggregate (SSD)	kg/m <sup>3</sup>	678	672	643	654

All mixtures were air entrained ranging from 4% to 8%

### *Material Constituents*

Type I/II Portland cement and Class C Fly ash was used. Air entrainment admixture was added to every mixture to target an air content between 4 and 8 percent. The fine aggregate was a natural sand graded within the limits specified by ASTM C33, and the coarse aggregate was a dolomitic limestone (crush). The coarse aggregate gradation for the 25 and 38 mm maximum size aggregate is shown in Table 2.

Table 2. Gradation and coarse aggregate characteristics

Sieve Opening	Coarse Aggregate 38 mm(1 1/2") max. size BSG=2.71 AC= 1.27%			Coarse Aggregate 25 mm ( 1") max. size BSG=2.67 AC= 2.0%		
	Retained (%)	Cumulative retained (%)	Cumulative passing (%)	Retained (%)	Cumulative retained (%)	Cumulative passing (%)
1.5"	0	0	100	0	0	100
1"	59	59	41	0	0	100
3/4"	34	92	8	33	33	67
1/2"	7	99	1	56	88	12
3/8"	1	100	0	9	97	3
#4	0	100	0	3	100	0
Total	100			100		

### PROPOSED METHOD TO CALCULATE SAW CUT DEPTH

There are five main steps required to calculate the timing and depth of the saw cut for jointed plain concrete: perform wedge splitting test, calculate fracture parameters from WST data, implement saw-cut depth model, calculate temperature curling stresses and determine saw cut depth for a given age.

#### *Wedge Splitting Test*

The Wedge Splitting Test was used to obtain the early age fracture properties of the concrete mixtures. Figure 1 shows the WST specimen geometry and dimensions, and also the loading configuration. The specimen has a cubic shape with a notch in the middle, generating a 113 mm deep ligament ( $a$ ) depth. This geometry is especially effective for early age testing due to the low self-weight effect and high ligament area. The specimen was supported on a thin steel bar and the horizontal splitting force ( $F_h$ ) is generated via the vertical force ( $F_v$ ) applied through the 10° steel wedge by using two metallic inserts with needle bearings. The crack opening ( $COD$ ) was measured on both sides of the sample using LVDT's that are located at the same height as the applied splitting force, which is 189 mm from the base of the sample.

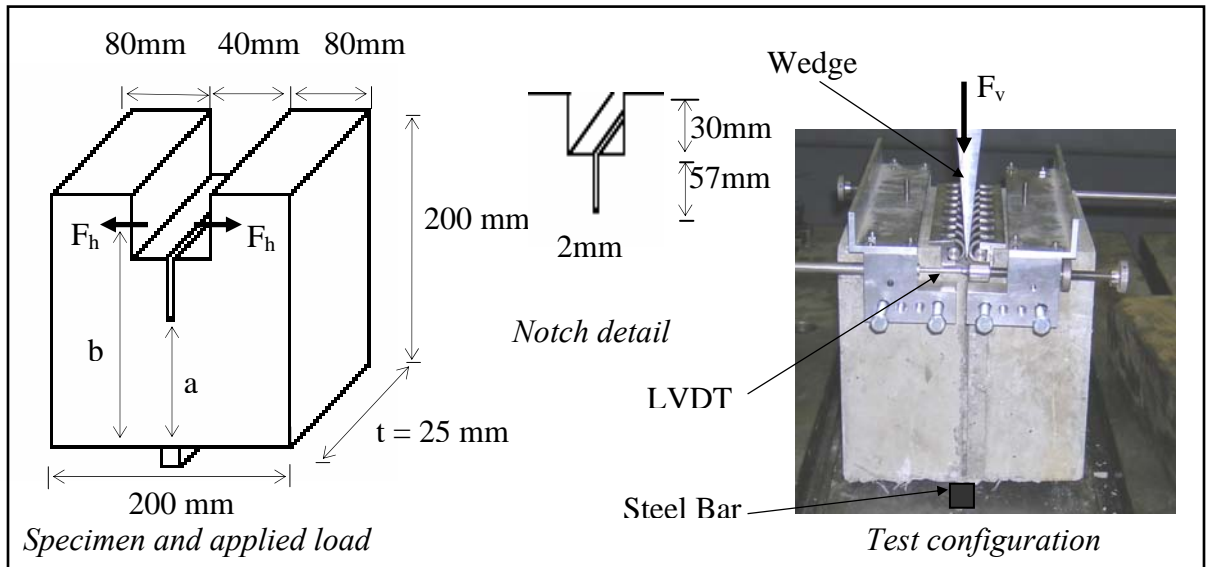


**Figure 1:** Wedge splitting test specimen and load configuration

The test is performed under vertical displacement control at a rate of 0.3 mm/min with the vertical load ( $F_v$ ) and COD collected at a frequency of 2 Hz. Two load-unload cycles are applied to each specimen, where each cycle loads the specimen until it reaches its peak and then unloads it immediately to zero. Figure 2 shows a splitting load versus COD plot obtained from one WST specimen. The splitting force ( $F_h$ ) is calculated from the vertical force as:

$$F_h = \frac{F_v}{2 \tan(\alpha)} \quad (1)$$

where  $\alpha$  is the wedge angle ( $10^\circ$ ). The purpose of the loading and unloading procedure is to propagate a crack and then determine the effective crack length based on procedure that was originally developed by Jenq and Shah [11] for the TPB specimen. The loading compliance ( $C_i$ ), shown in Figure 2, is calculated as the inverse slope from the splitting force versus COD loading curve on the first cycle, from 5 up to 40 percent of the peak force. The unloading compliance ( $C_u$ ) is obtained from the inverse of the slope of the splitting force versus COD unloading curve on the first cycle after the peak load is reached.  $C_u$  values are derived from the COD at 80 and 10 percent of the peak force.  $C_i$  and  $C_u$  are now used to calculate the effective crack length which can then be used to calculate  $K_{IC}$  and  $CTOD_c$ .

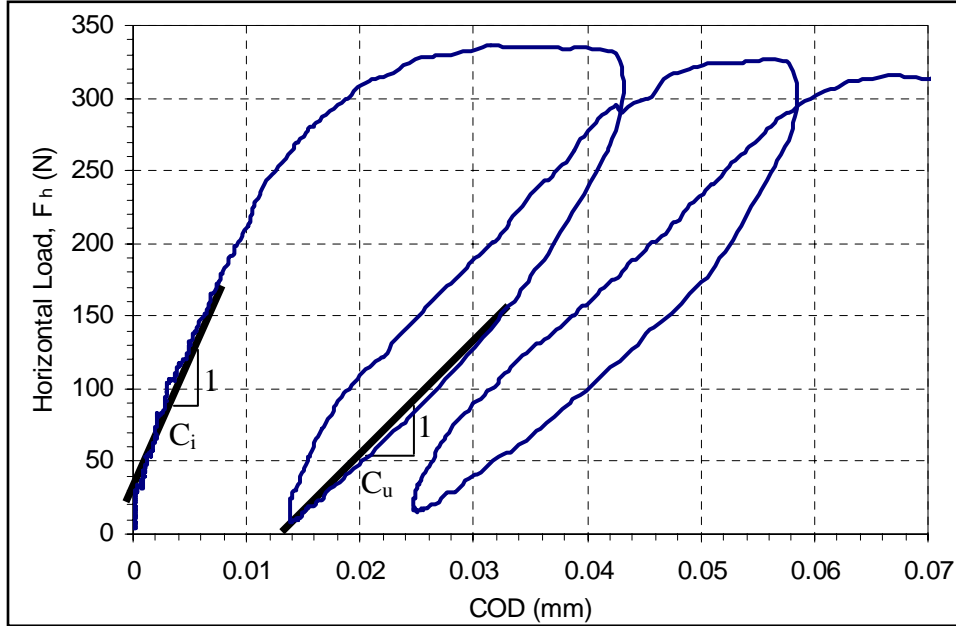


**Figure 2.** Horizontal Load vs. Crack Opening Displacement (COD) for two loading-unloading cycles, and the initial loading ( $C_i$ ) and unloading ( $C_u$ ) compliance.

### ***Calculation of Concrete Fracture Properties using WST results***

#### ***Wedge Splitting Test Fracture Equations***

In order to calculate the concrete fracture properties ( $K_{IC}$  and  $c_f$ ) from the experimental results obtained from the WST test, the effective crack length ( $a_c$ ) at the peak load must be determined. The  $a_c$  can be determined from finite element modeling of the WST specimen for various notch depths ( $a$ ) and matching the numerically determined compliance of the specimen with the experimental compliance. The basic principles of the two parameter fracture model (Jenq and Shah) [11], originally used with the TPB specimen, were followed to obtain the fracture properties of the concrete from the WST experimental results. The critical stress intensity factor ( $K_{IC}$ ) and critical crack extension ( $c_f$ ) are calculated by first obtaining the critical effective crack length ( $a_c$ ) at the peak load. This is completed by first equating the stiffness ( $E^*$ ) obtained with the loading and unloading compliance,  $E_i^*$  and  $E_u^*$ , respectively. The initial crack depth ratio ( $\alpha_0$ ) is calculated from the initial ligament ( $a = 113 \text{ mm}$ ) and the distance from the bottom of the specimen to the point where the load is applied ( $b = 189 \text{ mm}$ ) using:

$$\alpha_0 = \frac{a}{b} \quad (2)$$

The loading ( $E_i^*$ ) and unloading ( $E_u^*$ ) stiffness are calculated as:

$$E_i^* = \frac{f_2(\alpha_0)}{C_i * t} \quad (3)$$

$$E_u^* = \frac{f_2(\alpha_c)}{C_u * t} \quad (4)$$

where  $C_i$  is the loading compliance,  $C_u$  is the unloading compliance,  $t$  is the specimen width and  $f_2(\alpha)$ , is a geometric factor. Since the stiffness of the concrete does not change, just the effective crack length, equations (3) and (4) can be set equal to each other.

$$E_i^* = E_u^* = E^* \quad (5)$$

Therefore  $\alpha_c = a_c/b$ , ( $a_c$ ) may be obtained by solving iteratively equation (5). The Critical Stress Intensity Factor ( $K_{IC}$ ), Critical Crack Opening ( $COD_c$ ) and Critical Crack Tip Opening ( $CTOD_c$ ) can now be obtained from equations (6), (7) and (8), respectively.

$$K_{IC} = \frac{F_{hmax}}{t * b^{1/2}} f_1(\alpha_c) \quad (6)$$

$$COD_c = F_{hmax} \frac{f_2(\alpha_c)}{t * E^*} \quad (7)$$

$$CTOD_c = COD_c * f_3(\alpha_c) \quad (8)$$

where  $F_{hmax}$  is the peak splitting load,  $E^*$  is the stiffness obtained from equation (5),  $f_1(\alpha)$ ,  $f_2(\alpha)$  and  $f_3(\alpha)$  are geometric factors. Critical crack extension ( $c_f$ ) is related to the  $CTOD_c$  using the following equation proposed by Bazant and Becq-Giraudon [14]:

$$c_f = \frac{\pi}{32} \left[ \frac{CTOD_c * E^*}{K_{IC}} \right]^2 \quad (9)$$

#### *Finite element analysis and development of geometrical factors*

The geometric factors  $f_1(\alpha)$ ,  $f_2(\alpha)$  and  $f_3(\alpha)$  relate the specimen geometry with its compliance and fracture properties. Existing literature didn't provide those factors for the WST geometry used in this project. Therefore, the general purpose finite element package ABAQUS was used to perform a finite element analysis that allowed computing these factors. A two dimensional, plain strain model with a radial mesh around the crack tip was used to represent the WST sample. Figure 3 shows the global finite element mesh, the mesh around the crack tip, and the resultant geometrical factor equations. Q8 type elements with an average length of 10 mm were used far away from the crack tip, while collapsed Q8 elements with an average length of 2 mm and quarter nodes were used around the crack tip. The analysis was done using symmetry with the specimen sliced vertically and full restriction in the horizontal direction given.

The output of the finite element analysis (FEA) allowed for calculation of the WST geometric factors  $f_1(\alpha)$ ,  $f_2(\alpha)$  and  $f_3(\alpha)$ . These equations are obtained by running the FEM analysis for a fixed load at various crack depths ( $\alpha_i$ ). The values  $f_{1i}$ ,  $f_{2i}$  and  $f_{3i}$ , obtained for each crack depth ( $\alpha_i$ ) using equations (6) – (8), are plotted against  $\alpha_i$  and the equations are calculated by least square fit, as shown in Figure 3. Further details of the FEA model can be found in Villalobos [15].

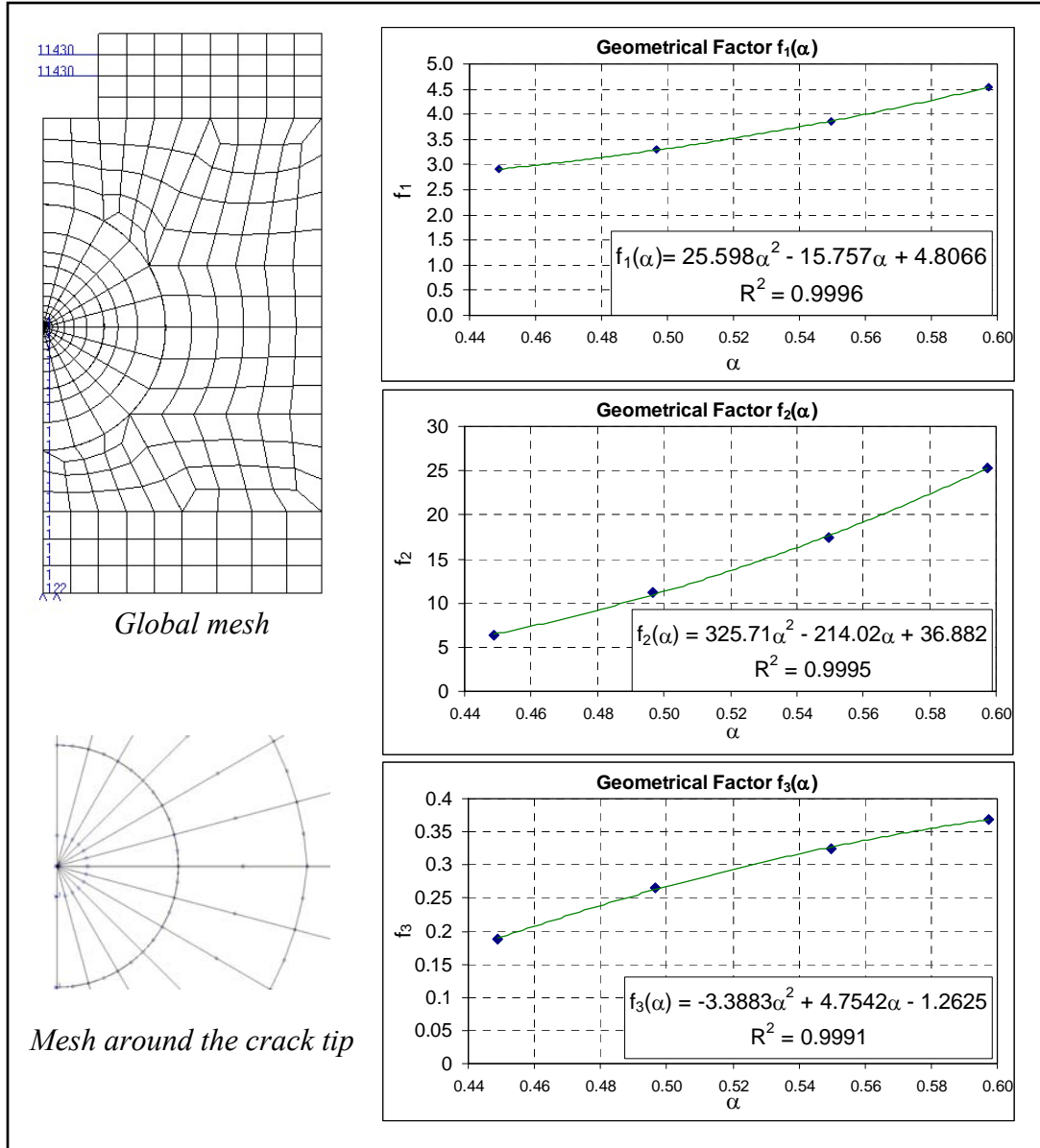


**Figure 3.** Global mesh, mesh detail and geometric factors for WST.

### Fracture Results

The critical stress intensity factor ( $K_{IC}$ ) for each mixture at ages ranging from 6 to 24 hours was obtained using the proposed formulation presented above. Table 3, in general, shows that the mixtures with lower cementitious content (555.44 and 555.44st) resulted in lower  $K_{IC}$  and larger coarse aggregate mixtures showed higher  $K_{IC}$  values. Table 3 also shows an increase in the critical crack extension ( $c_f$ ) until 12 hours which signifies the material has become less brittle (more quasi-brittle). After 12 hours,  $c_f$  tends to plateau which is consistent with previous research findings [4,10].

Table 3. Critical stress intensity factors and  $c_f$  values at early age.

AGE	MIXTURE			
	555.44	555.44st	688.38	688.38st
(hrs)	$K_{IC}(\text{MPam}^{1/2})$			
0	0.0	0.0	0.0	0.0
6	0.01	0.01	0.02	0.02
8	0.05	0.03	0.07	0.06
10	0.08	0.14	0.14	0.11
12	0.19	0.15	0.32	0.25
24	0.31	0.28	0.51	0.45
(hrs)	$c_f(\text{m})$			
6	0.001	0.003	0.002	0.001
8	0.005	0.008	0.007	0.004
10	0.006	0.008	0.012	0.006
12	0.006	0.023	0.024	0.018
24	0.007	0.017	0.021	0.017

### Saw-cut depth model

Once the concrete fracture properties are determined ( $K_{IC}$  and  $c_f$ ), the nominal strength of the concrete pavement for a given age and the thickness ( $d$ ) is calculated. The Size Effect Model (SEM) by Bazant [16], based on an effective elastic crack approach, has been used in the past for evaluation of saw cut requirements by Zollinger *et al* [2] and Soares [4]. The SEM enables the *nominal strength* ( $\sigma_n$ ) of the pavement to be calculated for any notch depths ( $a_o/d$ ) and slab thickness based only on the fracture properties ( $K_{IC}$ ,  $c_f$ ) of the concrete mixture and slab geometry:

$$\sigma_n = \frac{c_n K_{IC}}{\sqrt{g'(a_o/d)c_f + g(a_o/d)d}} \quad (10)$$

where  $\sigma_n$  is the nominal strength ( $P_{\max}/\text{width} \times \text{depth}$ ) of the concrete pavement that has a thickness equal to  $d$  and a saw-cut notch that has a depth equal to  $a_o$ .  $c_n$  is a factor related to the loading configuration. Soares [4] found through finite element analysis of a notched concrete slab that the stress intensity factors behaved similarly to a double edge notched tension specimen [DEN(T)] and thus the geometric factor [ $f(\alpha_o)$ ] for a DEN(T)

can be used. Since the  $f(\alpha)$  for a DEN(T) can be utilized,  $c_n$  is equal to unity for this loading configuration. The variable  $g(a_0/d)$ , called *nondimensional geometric function*, and its derivative  $g'(a_0/d)$  are convenient functions based on the notch depth ( $a_0/d$ ) and  $f(\alpha)$  and are described below:

$$g(a_0/d) = \pi \alpha c_n f^2(a_0/d) \quad (11)$$

$$g'(a_0/d) = \pi f^2(a_0/d) + 2\pi \alpha c_n^2 f(a_0/d) f'(a_0/d) \quad (12)$$

$$f(a_0/d) = 1.12 + 0.203(a_0/d) - 1.197(a_0/d)^2 + 1.93(a_0/d)^3 \quad (13)$$

$$f'(a_0/d) = 0.203 - 2.394(a_0/d) + 5.79(a_0/d)^2 \quad (14)$$

Equation (10) is valid for a notched pavement slab, i.e.  $a_0 > 0$ . The nominal strength on a notchless pavement slab ( $a_0 = 0$ ) should be calculated based on the Universal Size Effect Model [16] defined only for  $a_0 = 0$  as:

$$\sigma_n = \frac{c_n K_{IC}}{\sqrt{g'(a_0/d)c_f + g(a_0/d)d}} \left\{ 1 + \left[ \left( 0.5 + \frac{4g'(a_0/d)d}{1.4(-g''(a_0/d))c_f} \right) \left( 1 + \frac{g(a_0/d)d}{g'(a_0/d)c_f} \right) \right]^{-1} \right\} \quad (15)$$

where  $g'(a_0/d)$  and  $g''(a_0/d)$  are first and second derivative of  $g(a_0/d)$  as defined in equation (11), respectively.

The nominal strength can now be calculated from equations (10) to (15) for various notch depths ( $a_0/d$ ) and ages using the fracture properties given in Table 3. A family of curves representing different ages for each specific concrete mixture can be produced as seen in Figure 4 for 380mm slab thickness. Clearly increasing the notch depth ratio reduces the strength of the slab. To check the sensitivity of the nominal strength of the concrete slab to thickness, curves were also created for a slab thickness of 190mm as seen in Figure 5. As expected, the thicker slab actually produces lower nominal strength (see equation 10) which has been shown to be true experimentally by past researchers [16,19].

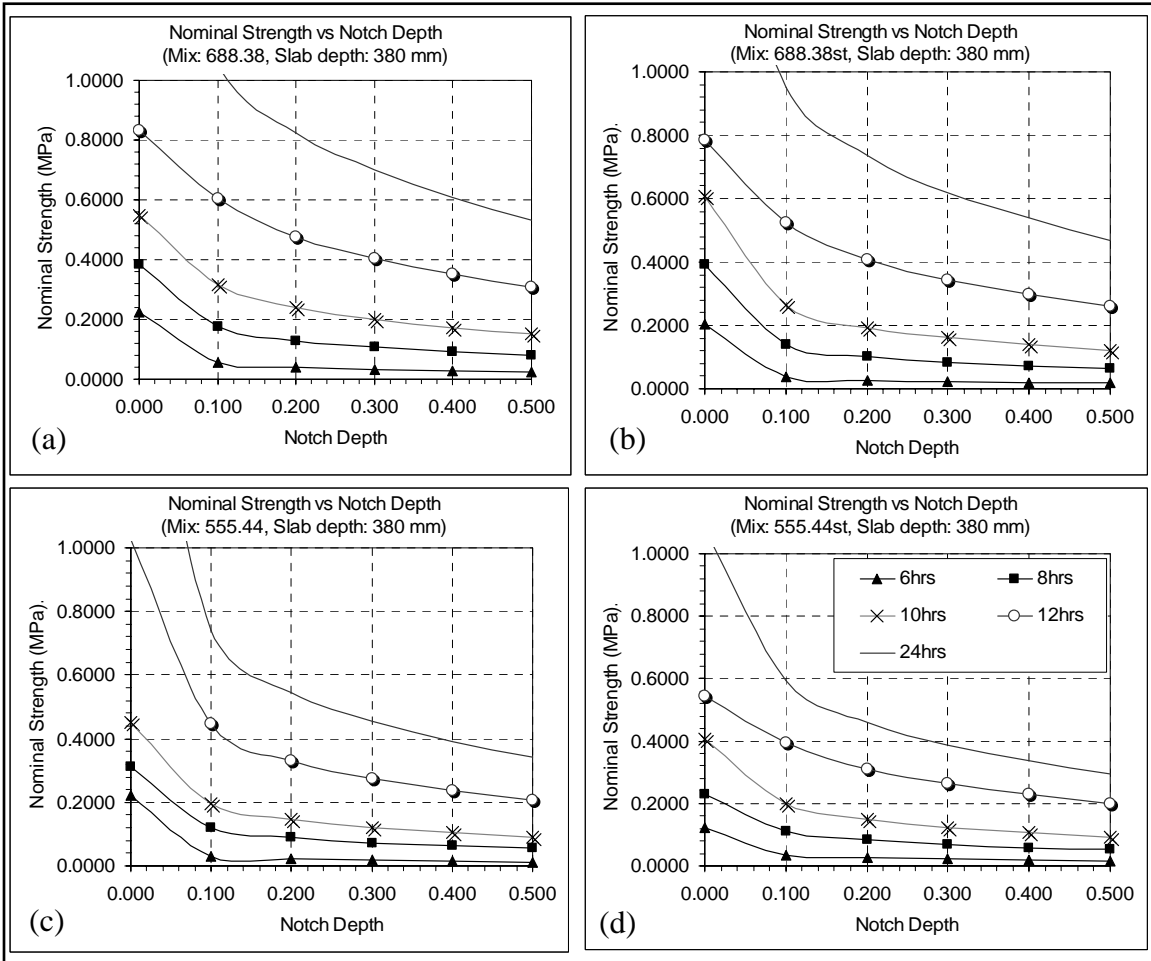


**Figure 4.** Nominal strength versus notch depth ratio for a 380 mm thick concrete pavement.

Figures 4 and 5 demonstrate that the nominal strength of the slab increases with age. The nominal strength also goes from highest to lowest in the following order: 688.38, 688.38st, 555.44 and 555.44st. The richer cementitious mixtures exhibit higher nominal strength, and the effect of the coarse aggregate size is more significant in this category, with a considerable increase in the nominal strength due the use of larger aggregates. The same trend is shown for the lean mixtures but at a smaller magnitude. The critical stress intensity factor has also a very important role on the nominal strength of the pavement, by increasing the rate of nominal strength growth especially at smaller ( $\alpha < 0.15$ ) notch depth ratios.

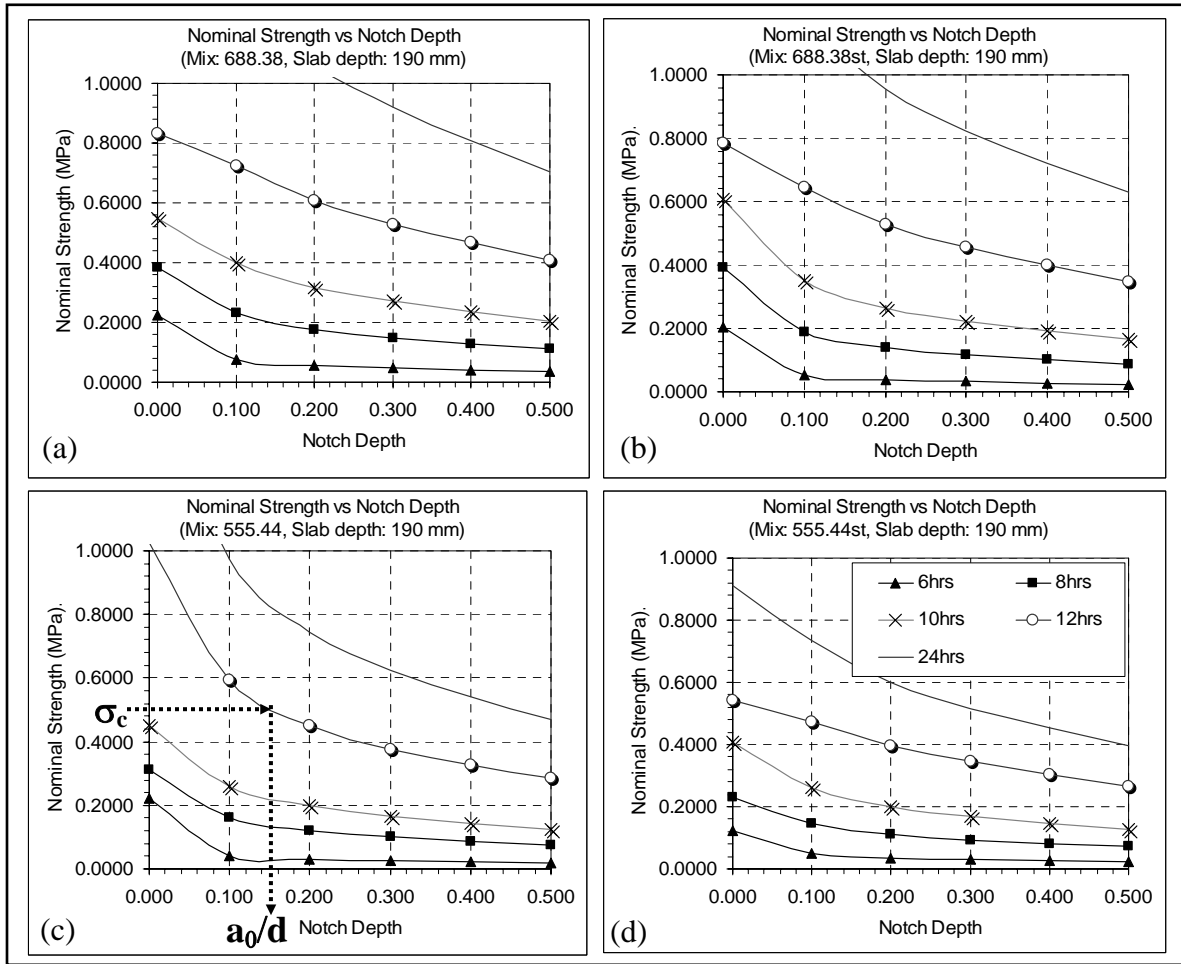


**Figure 5.** Nominal strength versus notch depth ratio for a 190 mm thick concrete pavement.

### *Temperature Curling Stress Calculation*

#### *Theoretical curling analysis*

In order to determine the required notch depth ratio for any given age, the maximum applied stress in the pavement must be calculated. In the first 24 hours, temperature stresses predominate assuming autogenous shrinkage is kept to a minimum by choosing a moderate water-cement ratio. The temperature curling stress can be calculated using Westergaard equation [17] for a semi-infinite strip slab (similar to a new pavement without any discrete joints) resting on a Winkler foundation:

$$\sigma_c = \frac{C_a E \alpha_T \Delta T}{2(1-\nu)} \quad (16)$$

where  $\sigma_c$  is the maximum tensile stress (MPa),  $E$  is the modulus of elasticity of the concrete (MPa),  $\alpha_T$  is the coefficient of thermal expansion ( $1/^\circ\text{C}$ ) and  $\Delta T$  is the

temperature difference through the slab (°C).  $C_a$  is a geometric correction factor proposed by Bradbury [18] defined as:

$$C_a = 1 - \frac{2 \cos \lambda \cosh \lambda (\tan \lambda - \tanh \lambda)}{\sin 2\lambda \sinh 2\lambda} \quad (17)$$

$$\lambda = \frac{L}{l\sqrt{8}} \quad (18)$$

and  $l$  is the radius of relative stiffness described by:

$$l = \sqrt[4]{\frac{Ed^3}{12(1-\nu^2)k}} \quad (19)$$

where  $E$  and  $\nu$  are the modulus of elasticity and Poisson's ratio of the concrete, respectively,  $d$  is the slab thickness,  $L$  is the width of the slab and  $k$  is the modulus of subgrade reaction.

#### *Curling stress example*

Two pavement designs are presented as examples to compare the saw cut depth requirements in a thin (0.19 m) and a thick (0.38m) concrete pavement structure. These pavements are built over a subgrade with a  $k$  of 40.7 MPa/m (150 psi/in). The concrete used in this example has a Poisson's ratio ( $\nu$ ) of 0.15 and a thermal expansion coefficient of  $9 \times 10^{-6}/^\circ\text{C}$ . The values for modulus of elasticity ( $E$ ) have been estimated based on early age compressive strength data and are presented in Table 5.

Table 4. Estimated elastic modulus at early ages

AGE(hrs)	6	8	10	12
MIXTURE	Elastic Modulus(MPa)			
555.44	3,329	4,369	5,409	6,449
555.44st	2,917	3,961	5,005	6,050
688.38	3,188	4,184	5,180	6,176
688.38st	3,343	4,537	5,731	6,925

The curling stresses for each was calculated for a 5.71 m (18.75 ft) and 4.57 (15.00 ft) wide strip slab, for the 0.38 and 0.19 m pavement thickness, respectively (e.g., airport and highway rigid pavement, respectively). It is also known that the temperature differential is less in a thinner slab, therefore, a  $\Delta T$  of 10 and 8 °C will be used for the 0.38 and 0.19 m pavement, respectively (temperature top is less than the temperature bottom). The tensile stresses for each slab, mixture and age combination are presented in Table 5. The curling stresses are similar for each age since the coarse aggregate and sand source is the same and only effect the elastic modulus of the concrete.

Table 5. Top tensile stresses due temperature curling at different ages and slab thickness

Tensile Stress (MPa)								
AGE(hrs)	6		8		10		12	
Slab depth (m)	0.19	0.38	0.19	0.38	0.19	0.38	0.19	0.38
555.44	0.15	0.18	0.20	0.23	0.25	0.28	0.30	0.32
555.44st	0.13	0.16	0.18	0.21	0.23	0.26	0.28	0.30
688.38	0.15	0.18	0.19	0.23	0.24	0.27	0.28	0.31
688.38st	0.15	0.18	0.21	0.24	0.26	0.29	0.32	0.34

### *Age and Thickness Dependent Saw Cut Depth*

The required saw-cut depth for a given age is obtained by using the curling stress ( $\sigma_c$ ) from Table 5 as an input to corresponding nominal strength ( $\sigma_n$ ) chart for the specific concrete mixture (Figures 4 and 5). As shown in Figure 5 for mix 555.44 at 12 hours, a horizontal line has to be extended at a value equal to  $\sigma_c$  until intersecting the 12 hour curve. The x-value from the intersection point is the minimum recommended notch depth at that concrete age. Table 6 summarizes the recommended saw cut depth for a given slab thickness, concrete mixture, and concrete age. If the notch depth is too shallow or the temperature curling stress is higher than the nominal strength, the concrete will have a higher probability of random cracking. The recommended saw cut depth presented in Table 6 are visually summarized in Figure 6.

Table 6. Recommended saw cut depth for 4 concrete mixtures at various ages

Saw Cut Depth ( $a_0/d$ )								
AGE(hrs)	6		8		10		12	
Slab depth (m)	0.19	0.38	0.19	0.38	0.19	0.38	0.19	0.38
555.44	0.04	0.02	0.07	0.03	0.11	0.06	0.47	0.21
555.44st	0.01	0.01	0.05	0.01	0.12	0.06	0.46	0.22
688.38	0.05	0.02	0.16	0.06	0.38	0.14	0.71	0.49
688.38st	0.03	0.02	0.09	0.05	0.21	0.09	0.56	0.37

The most significant factor from Figure 6 is the effect of the concrete age. The recommended saw cut depth increases dramatically after 10 hours for the concrete mixtures evaluated. This observation also agrees with other investigation where is mentioned that in field tests the vast majority of the cracking of a notched pavement structure initiates between 11 to 12 hours after the material was placed [3].

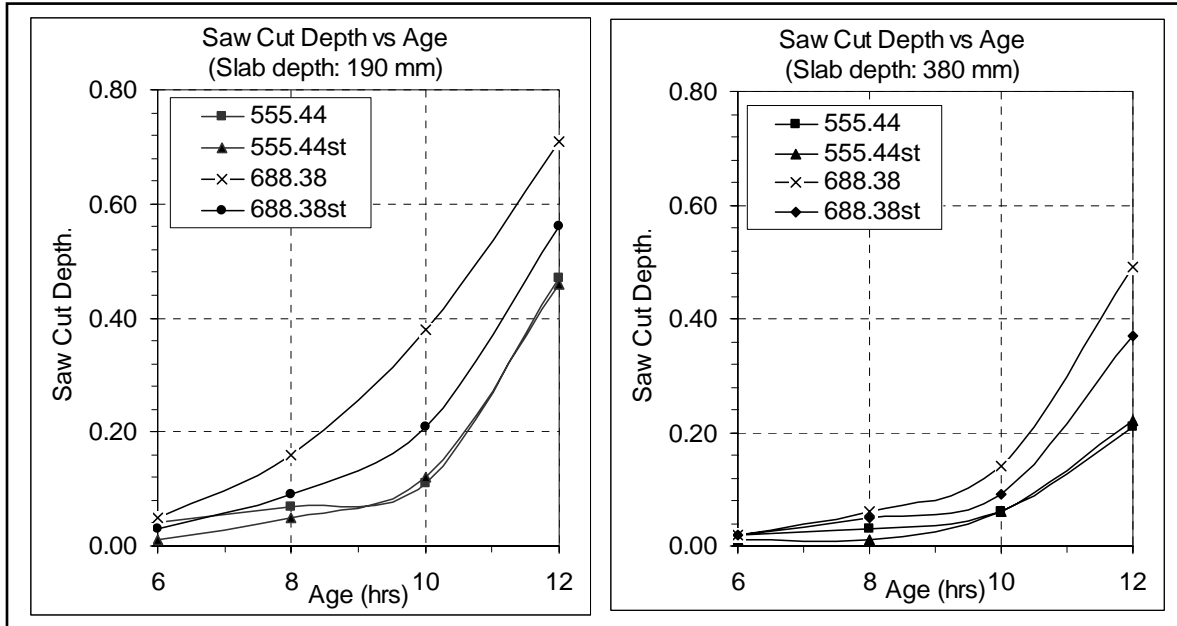


**Figure 6.** Saw cut depth versus age for slab thickness of 190 and 380 mm.

The concrete mixture design has an impact on the required saw cut depth of the pavement. This can be seen in Figure 6, where both concrete mixtures with high cementitious content (688.38 and 688.38st) require greater saw cut depths than the mixtures with lower cementitious content (555.44 and 555.44st). The higher cementitious mixtures has greater fracture properties at a given age and thus more energy is needed to propagate the crack for a given notch depth. Mixture 688.38, which has the 38 mm coarse aggregate size also needs a higher saw cut depth relative to the 25mm coarse aggregate size (688.38st). The coarse aggregate size is negligible for mixtures 555.44 and 555.44st, which could be related to the weaker aggregate-paste interface.

As seen clearly in Figure 6, thinner concrete pavements require significantly deeper notch depth ratios relative to thicker slabs. The average notch depth ratio for the 0.19 m pavement is almost twice the minimum requirement for the 0.38 m pavement. This difference is a result of the combined effect of the higher nominal strength and lower curling stresses on thinner pavements.

The theoretical analysis and practical example lead to the observation that if more time is desired to saw-cut the concrete pavement than a concrete with slower developing fracture properties should be selected. Furthermore, concrete mixtures with larger aggregate sizes and higher cementitious contents will require considerably deeper notches if timing is delayed. As seen in Figures 4 and 5, if the saw cut is preformed at an earlier age (i.e. 6 to 8 hours) the depth can be smaller than the typically specified  $d/3$  or  $d/4$ .

## CONCLUSION

A procedure was developed to calculate saw cutting requirements based on fracture parameters derived from the wedge splitting test (WST) setup. Finite element analysis of the WST configuration was completed in order to obtain the necessary geometric factors required to calculate the early-age fracture properties [*Critical Stress Intensity Factor ( $K_{IC}$ )* and *Critical Crack Extension ( $c_p$ )*] from the experimental data. An existing saw cut depth model was modified to analyze the effect of changes in concrete mixture constituents and slab geometry. Results show that saw cutting depth requirements on a given pavement, typically 1/4 or 1/3 of the slab depth, can significantly vary depending on the timing, the cementitious content, and the size of the coarse aggregate.

For the concrete materials characterized in this study, the saw cut model predicted a dramatic increase in the required notch depth after 10 hours for all mixtures. The concrete mixtures that exhibited higher fracture properties at early ages required deeper saw cut depths. The concrete mixtures with higher cement contents (688.38 and 688.38st) required deeper saw cut notches relative to the mixtures with lower cement content (555.44 and 555.44st). The larger aggregate size with higher cementitious content required a deeper notch depth for a fixed age. Thinner concrete pavements sections (190mm) were also more sensitive to saw cut depth and timing relative thicker rigid pavements (380mm). The amount of variables affecting saw cut depth and timing suggests that it should be determined once the material constituents and environmental conditions are known, not during the initial pavement design.

## REFERENCES

1. Federal Airport Administration, "Airport Pavement Design and Evaluation, Advisory," Circular 150/5320-6D, Federal Aviation Administration, Washington, D.C., 1995.
2. Zollinger D.G., Tang T., and Xin D. "Sawcut Depth Considerations for Jointed Concrete Pavement Based on Fracture Mechanics Analysis". *Transportation Research Record*, No. 1449, TRB, Washington, D.C., 1994, pp. 91-100.
3. Jeong, J.H., Chapke, N., Zollinger, D.G., "A Probabilistic Approach to Saw Cut Timing and Saw Cut Depth Requirements for Newly Constructed Portland Cement Concrete Pavements," *7<sup>th</sup> International Conference on Concrete Pavement*, Orlando, Florida, USA, September 9-13, 2001.
4. Barbosa-Soares, J., "Concrete Characterization Through Fracture Mechanics and Selected Pavement Application," *Ph. D Thesis*, Department of Civil Engineering, Texas A&M University, December 2003
5. Zollinger, D.G., Tang, T. and Yoo, R.H., "Fracture Toughness of Concrete at Early Ages," *ACI Materials Journal*, Vol. 90, No.5, 1993, pp. 463-471.

6. Jensen E.A., and Hansen W. "Fracture Energy Test for Highway Concrete: Determining the Effect of Coarse Aggregate on Crack Propagation Resistance". *Transportation Research Record*, No. 1730, TRB, Washington, D.C., 2000, pp. 10-17.
7. Bazant ZP, Kazemi MT. "Determination of fracture energy, process zone length and brittleness number from size effect, with application to rock and concrete", *International Journal of Fracture* 1990, Vol44, pp.111-131.
8. Tschegg, E.K. et al, "Fracture Mechanical Behavior of Aggregate-Cement Matrix Interfaces," *Journal of Materials in Civil Engineering*, 1995, pp. 99-203.
9. Brühwiler and F. H. Wittmann, "The Wedge Splitting Test, a New Method of Performing Stable Fracture Mechanics Tests," *Engineering Fracture Mechanics*, Vol. 35, 1990, pp. 117-125.
10. Østergaard, L., "Early - Age Fracture Mechanics and Cracking of Concrete," *Ph. D Thesis*, Department of Civil Engineering, Technical University of Denmark, 2003
11. Jenq, Y. S., and Shah, S. P.. "Two parameter fracture model for concrete." *ASCE J. Eng. Mech.*, 111(10), 1227-1241., 1985.
12. Roesler, J.R., Gaedicke, M.C., "PCC Mix Design". *Technical Note 2 – Center of Excellence of Airport Technology*, University of Illinois at Urbana Champaign, 2005.
13. Roesler, J., Gaedicke, C., Lange, Villalobos, S., Rodden, R., and Grasley, Z., "Mechanical Properties of Concrete Pavement Mixtures with Larger Size Coarse Aggregate," *ASCE 2006 Airfield and Highway Pavement Conference*, Atlanta, GA, 11 pp. 516-527, 2006.
14. Bazant, Z. P., and Becq-Giraudon, E. "Statistical prediction of fracture parameters of concrete and implications for choice of testing standard." *Cement and Concrete Research*, 32(4), 529-556, 2002.
15. Villalobos-Chapa, S., Fracture Properties of Concrete and Determination of Saw-Cut Timing and Saw-Cut Depth of Concrete Pavements, *MS Thesis*, University of Illinois, Urbana, IL, 2006.
16. Bazant, Z. P., Planas, J. "Fracture and Size Effect in Concrete and other Materials", *CRC Press*, NY, 1997.
17. Westergaard, H.M., "Analysis of Stresses in Concrete Roads Caused by Variations of Temperature," *Public Roads*, Vol. 08, No. 03, May, pp. 54-60, 1927.
18. Huang, Y.H., "*Pavement Analysis and Design*", Prentice-Hall, NJ, 1993.

19. Roesler, J.R., "Fatigue Resistance of Concrete Pavements," *6th International DUT – Workshop on Fundamental Modelling of Design and Performance of Concrete Pavements*,